

# ACOUSTIC LEVITATION BY A METAMATERIAL-BASED CLOAK

Mohd Adili Norasikin, Gianluca Memoli, Diego Martinez Plasencia and Sriram Subramanian

*University of Sussex, School of Engineering and Informatics, Falmer, UK  
email: m.norasikin, g.memoli, d.martinez-plasencia, sriram @sussex.ac.uk*

Acoustic levitation is historically achieved using two opposite arrays of transducers, but examples using single-sided “bottle-shaped” or “tripod-like” traps also exist in the literature. In these realisations, however, a compromise needs to be found between the Nyquist theorem (which would force the space between transducers below half-wavelength, to avoid spatial aliasing effects) and the cost of smaller transducers, thus limiting practical applications. In this study, we use low-cost 3D printed labyrinthine metamaterial bricks, assembled in front of the source, to create a new type of trap, based on the concept of acoustic cloak. This solution is potentially much cheaper than an array-based one and may allow levitate objects larger than the wavelength with relative low power, as the shaping mechanism is separated from the generation one. In particular, we let the acoustic energy flow along a pre-determined three-dimensional closed curve, generating equilibrium state of energy force at the end of the curve to suspend object in air. We take the uniform-phase wave generated from a 16x16 array of 10mm transducers (40kHz in air) as input to a metamaterial layer made of pre-manufactured bricks, arranged perpendicularly to the direction of propagation. Each brick is half-wavelength in size and is designed to encode a particular phase. After validating the concept through COMSOL simulations and microphone scans on a trap, we present some preliminary results on levitation.

Keywords: (e.g. acoustic levitation, metamaterial, acoustic cloak)

---

## 1. Introduction

Acoustic levitation technologies offer interesting capabilities of levitating substance in air and profoundly significance in biomaterials [21], pharmaceuticals [22] and microparticles [6] studies.

Historically, acoustic levitation was first achieved in standing waves [3], in a “transducer-reflector” arrangement where particles get trapped in the acoustic pressure nodes. The principle behind this acoustic set-up is reliable and leads to strong trapping forces, which is why it is at the core of advanced graphics and display [15, 16, 18] applications. In the years, transducer-reflector arrangements have been exploited to levitate and handle different substances in air, including living like insects [23] or fish embryos [20]. This configuration starts to fail when more control on the levitated matter is desired (e.g. movement): not only the spacing between the traps is limited to half-wavelength  $\lambda/2$ , but the whole standing wave needs to shift for a single trap to be displaced.

The typical solution is to use transducer arrays: in “acoustic tweezers” [2, 8, 9] set-ups, precise control on the phase of each transducer allows dexterous control of one or multiple traps. Typically, at least two pressure focal points are used to levitate substances against gravity. A variation of this set-up (i.e. “tractor beam” set-ups) even achieved manipulation of substances in air using a single-sided transducer array [12–14]. These set-ups have in common three main limitations: forces are relatively smaller in the plane perpendicular to gravity, size of the levitated particles is limited to half wavelength (due to diffraction) and, when transducers are larger than  $\lambda/2$ , are subject to energy losses due to aliasing effects (Nyquist theorem).

The literature reports two other interesting arrangements for acoustic levitation: a “tripod-like” set-up, which has been recently used to levitate a large polystyrene sphere (50mm in diameter)[1], and a “ $\lambda/2$  trap” set-up, which has been used to levitate a compact disk on top of a 19kHz transducer [26]. Despite these two methods successfully levitated large object, the distance between the transducer(s) and the levitated object was approximately half-wavelength. Additionally, in the case of the levitated CD, a rod was being used to stabilize the levitated object in acoustic field thus decrease the system versatility.

In this study we address the limitations in size and distance from the source by combining the concept of acoustic cloaking [27] with the one of acoustic meta-materials [5]. Acoustic cloaking exploits the properties of diffraction and interference to create areas with no acoustic pressure in an otherwise fully operating acoustic field and, because of that, has already been suggested as a possible technique for transducer-array based levitation [24]. In this study, we build on the cloaking idea but act differently: we project acoustic energy in the far field by steering sound waves along a pre-determined curve in the near field, in cylindrical symmetry, thus forming an acoustic trap at the end of it. We then apply simple phase distributions to stretch the curve, thus moving the trap vertically, just like a car jack lifts a vehicle while changing a wheel (“car-jack” set-up).

Our preliminary explorations, not discussed here, have shown however that such a degree of control is not achievable when the transducers are larger than the wavelength, which is the typical situation at 40-80 kHz. For this reason, we used low cost 3D printed labyrinthine metamaterial bricks[14] to produce the cloak, assembled in front of 40kHz ultrasound array, leaving to the array only the role of steering device. With this arrangement, we managed to levitate different substances, as large as one wavelength ( $\lambda \approx 8.58\text{mm}$ ), at distances ranged from  $5\lambda$  to  $10\lambda$ . We discuss the benefits and the limitations of our set-up, highlighting how the concept leads to future applications.

### 1.1 Acoustic cloaking: basics and impact on levitation

Acoustic cloaking is a well-studied method to bend acoustic waves along a pre-designed curve [10, 24, 25], with applications in building insulation and noise management [11] and even earthquake protection [4]. The key side effect of producing a low-pressure area, which makes it surrounded by high-pressure regions, gives to acoustic cloaking a huge potential for levitating objects in air. Zhang et al. [24] looked into this, successfully confining acoustic energy along the self-bending curve of an acoustic cloak and demonstrating how the curved trajectory is designable from any uniformly curved arc. These authors also reported that the curved beam has the ability to self-reconstruct when it is bends around an obstacle. These two findings show the possibility to levitate at the end of the arc (where the acoustic rays converge during reconstruction), pushing matter up like in the “tripod-like” set-up [1], but offering full cylindrical symmetry and a potentially a stronger radial confinement.

Following the technique described by Zhang *et al.* [24], we design the cloaking curve using cubic Bezier with four control points, obtaining a curve  $x = f(z)$  – see Fig. 1(a). If  $(x_i, z_i)$  are the coordinates of the Bezier points and  $t \in [0,1]$ , the curve in parametric form appears like:

$$x(t) = (1-t)^3x_0 + 3(1-t)^2tx_1 + 3t^2(1-t)x_2 + t^3x_3 = h(t) \quad (1)$$

$$z(t) = (1-t)^3z_0 + 3(1-t)^2tz_1 + 3t^2(1-t)z_2 + t^3z_3 = g(t) \quad (2)$$

Consequently,

$$f = h \circ g^{-1}(t) \quad (3)$$

and from this relation we obtain  $f'(z)$  and  $f''(z)$ , which are both quotients of polynomials. Within the approximations of ray acoustics, we obtain from this curve the geometrical wave-front  $(u(x, z), v(x, z))$  perpendicular to acoustic source, assumed at  $z = 0$ .

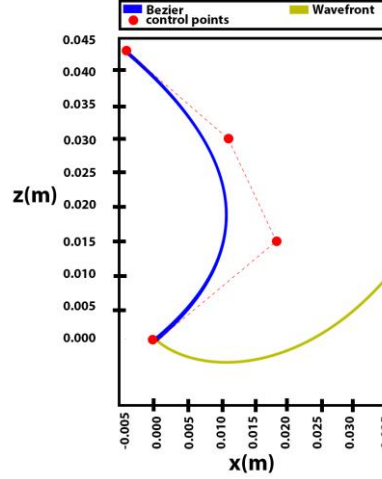


Figure 1: Pre-designed Bezier curve. Highlighted in the picture are the 4 control points (red dots), the parametric Bezier – blue line, from Eqq. (1) and (2) – and the wave front necessary to achieve it – yellow line, from GQ. (4) and (5). Acoustic radiation propagates towards z-axis direction, in this picture.

It can be shown that [24]:

$$u(z) = \frac{I(z) + C(z_0)}{\sqrt{1 + (f'(z))^2}} - f'(z) \cdot \frac{f(z) - zf'(z)}{1 + (f'(z))^2} \quad (4)$$

$$v(z) = \frac{f'(z) \cdot I(z) + C(z_0)}{\sqrt{1 + (f'(z))^2}} + \frac{f(z) - zf'(z)}{1 + (f'(z))^2} \quad (5)$$

where

$$I(z) = \int_{z_0}^z \frac{(f(z) - zf'(z))f''(z)}{(1 + (f'(z))^2)^{3/2}} dz \quad (6)$$

$$C(z_0) = \frac{(z_0 + f'(z_0)) \cdot f(z_0)}{\sqrt{1 + (f'(z_0))^2}} \quad (7)$$

In this paper, we achieve the geometrical self-accelerating beam by imposing a phase distribution on an assembly of metamaterial bricks, each of which encodes a specific phase delay between 0 and  $2\pi$  [14]. The required phase profile  $\varphi(x)$  is determined by the following parametric equations:

$$x = v + u \frac{du}{dv} \quad (8)$$

$$\varphi = ku / \cos(\arctan(-du/dv)) \quad (9)$$

where  $k = 2/\pi\lambda$  is the wave number.

At this point, the size of the transducers becomes crucial: the spatial sampling needs to be at least smaller than  $\lambda/2$ , according to the Nyquist theorem. As will be discussed in the next section, our selected brick size was just compliant with this fundamental limit: assembling them in a metasurface allowed us to separate geometrical shaping from trap control. Zhang *et al.* [24], in fact, used back-propagation to Fourier-transform the phase  $\phi(x, 0)$  into  $\phi(x, -z_0)$ , de facto moving the Bezier curve at a distance  $z_0$  from their transducer array and assigning on it a more complex phase distribution. We decided instead to exploit some results already known in holographic optical tweezers, encoding on the transducer array a combination of a diffraction grating and a Fresnel lens [17, 19].

Using optical formulae in a simplified version, encoding the phase distribution

$$\varphi_s(x, y) = \underbrace{B[x x_{to,1} + y y_{to,1}]}_{\text{Diffraction grating}} + \underbrace{Az_{to,1}[x^2 + y^2]}_{\text{Fresnel lens}} \quad (10)$$

should produce a shift of the trap in three dimensions, where  $x$  and  $y$  are the cartesian coordinates on the phased array (calculated from its center),  $\lambda$  is the wavelength of the sound,  $A$  and  $B$  are user-controlled constants, while  $[x_{to,1}, y_{to,1}, z_{to,1}]$  are the desired position of the trap.

## 2. Materials and methods

As discussed in the previous section, our trapping set-up consists of two main parts: an array of meta-material bricks, assembled in a meta-surface, and a transducer array operating at 40 kHz (Fig. 2). In this setup, a trap will be created using the static metamaterial bricks, just on top of the meta-surface, and will be then displaced further down in the field using the transducers array on the board (“car-jack” set-up). Our source is an Ultrahaptics board (Ultrahaptics, Bristol, version 2.0.0), that consists of 16x16 40 kHz close-packed transducers (radius: 5mm, lateral separation: 10.5mm, nominal emission 120 dB). The board is programmed using SDK version 1.2.4., using an in-house control software written in C++ (xCode version 8.3.2). It is important to note that, as confirmed by experiments and simulations not reported here, these transducers are not able to create a self-bending curve, due to the large aliasing effects [6, 20, 22] due to their size.

We overcome this limitation with the second part of the setup: metamaterial bricks [12]. We use 16 types of bricks, all optimised for high transmission at 40 kHz, each encoding a different phase delay between 0 and  $2\pi$ . The bricks were produced by rapid prototyping (ProJet HD 3000 Plus printer) and the labyrinthine features inside them were at the limit resolution of the process, while their lateral size was chosen to be half wavelength. The closed curve in Fig. 1(a) was obtained using a holder (laser-cut in acrylic using Universal Laser System VSL, version 2.3) that allocated a grid of 24x24 bricks as in Fig. 2(b) the phase distribution for the self-bending acoustic curve in Fig. 1 was computed using a Python 2.7 program based on Eq. (1-9), and the result appears in Fig. 3(a). In order to design a radial curve, we selected the central axis of the grid in Fig. 2(b) and computed the Euclidean distance, which was assimilated to the  $x$  coordinate in Fig. 3(a). Quantisation of the meta-surface in the phase domain was achieved by selecting the brick with the nearest phase to the desired one.

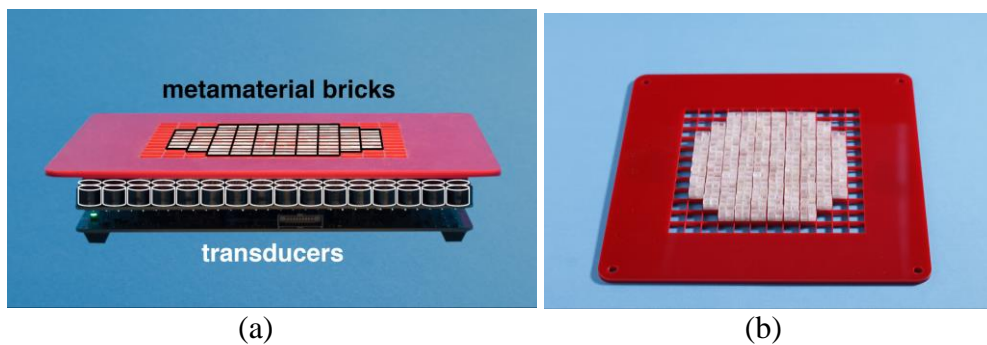


Figure 2: Experimental setup used in this study. (a) Hybrid arrangement and (b) metasurface producing the static acoustic cloak

## 3. Results

### 3.1 Simulations and characterisation of the trap

The output of the system in different configurations of the input parameters was simulated using the Acoustic module in COMSOL Multiphysics (COMSOL, Cambridge, UK, version 5.2a). Exploiting the cylindrical symmetry, 2D simulations run on an iMac workstation (3.4 GHz Intel Core

i5 processor, 16GB DDR3 ram, macOS Sierra version 10.12.5 operating system). Figure 3(b) shows, in particular, the simulated SPL using the parameters in Fig. (1) and Fig. 3(a), when the phase of the transducers array was uniform.

Simulations were verified using an in-house built scanning system, based on a commercial 3D printer set-up, piloted by a C++ custom code. Measurements were conducted acquiring the readings of a B&K microphone (model 4138-A-015) through a conditioning amplifier (Nexus, final gain of the chain: 3.16V/Pa), using a PicoScope (Pico Instruments, model: 5444b). In particular, Fig. 3(c-e) illustrate horizontal scans (4mm resolution) across the un-displaced Bezier curve at three different positions along the  $z$  axis ( $z=40\text{mm}$ ,  $50\text{mm}$ , and  $60\text{mm}$ ). A quick comparison with Fig. 3(b) confirms the desired bending, but also shows a leaking of acoustic energy along the axis. The asymmetry of the circle of high pressure suggests a potential issue with the parallelism between the transducer array and the planar structure that holds the bricks. Another potential reason for this asymmetry comes from the holding structure itself: we realised, *a posteriori*, that some of the bricks were slightly misaligned due to errors in manufacturing.

As shown in Fig. 3(f), we also used solid  $\text{CO}_2$  (i.e. dry ice) for a quick visualisation of the acoustic field. The vapours produced during sublimation highlighted the lines of the field, allowing a quick evaluation of different experimental conditions. This was particularly useful when the Bezier curve was displaced using the transducer array.

### 3.2 Experiments with a displaced trap

Fig. 4 reports a summary of our experiments with a displaced trap. In this study, we limited our tests to vertical displacements, which were achieved by changing the parameter  $A$  in Eq. (10) between  $2\pi$  to  $6\pi$ . A comparison of the simulations in Fig. 4 (a-c) with the trap before displacement – Fig. 3(b) – show the Bezier elongating in the  $z$  direction as  $A$  is increased, thus pushing the self-reconstructed high-pressure region upwards. This prediction was confirmed by the measurements in Fig. 4 (d-f), where the intensity of the high-pressure region is so strong that the Bezier is barely visible. Fig. 4(g-i) demonstrate the principle of our “car-jack” trap, showing an object trapped on top of the high-pressure region, moving alongside the displaced trap.

### 3.3 Levitation of different objects

We probed the manipulation capability of our set-up by setting  $A = 6\pi$  and levitating objects of different size and material, but with a common weight of 5 mg. In particular, as shown in Table 1, we managed to levitate as large as one wavelength. We also observed that, as the volume of the levitated object increased, its levitated position increased. This behaviour has to be expected: since the pressure needed to levitate an object depends primarily on its density, objects with higher pressure move closer to the high-pressure core below the trap, where the acoustic force is large enough to balance their density.

## 4. Discussion

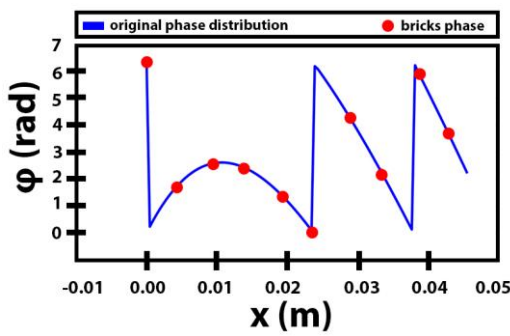
Figure 4 shows a low-energy region surrounded by high-energy at  $x \approx 55\text{-}60\text{ mm}$  (i.e. our acoustic cloak), which seems to be a perfect region for a trap. However, we were not able to levitate inside the cloak because of the leaked energy. This leakage would affect not only stability of the trapped object, but also accuracy of experimental measurements.

A possible way to make alignment problems less crucial would be to have control over amplitude [20], which we lack in the current setup. We also observed that misalignment of the metamaterial bricks may have a significant impact on acoustic field, so that future realisations of this trap will need to ensure better control over this factor.

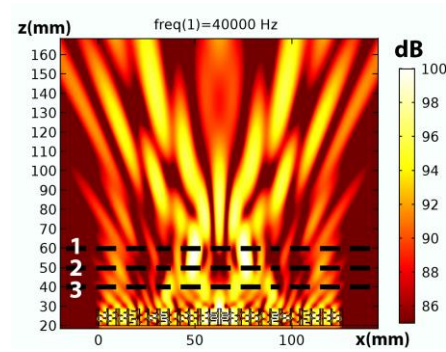


## 5. Conclusion and future works

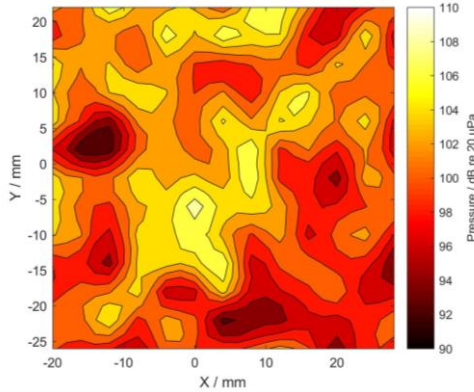
In this work, we presented a trapping system based on the combination of a self-bending beam and metamaterials. We used fixed metamaterials to produce a stable trap, that was then displaced vertically encoding an appropriate phase on the transducer array. We conducted numerical simulations and experimental measurements and demonstrated the capabilities of our levitation setup to shift the trap in the vertical direction. With this set-up, we managed to levitate different objects with size at least comparable with the wavelength. In future works, the amplitude will be manipulated in order to provide even distribution of energy of generated acoustic field. A linear phase should be introduced on top of the parabolic phase to skew the acoustic field and possibly move the trap left and right. A thicker and strong material should be used to hold the bricks and reduce misalignment. A program will be built to control the trap position in real-time. Finally, a bigger trap can be produced by changing the size of acoustic cloak, hence increasing the levitated object size.



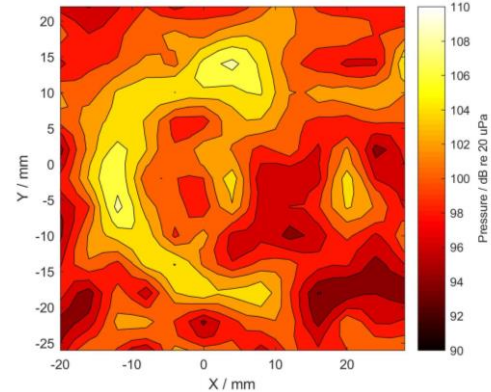
(a) Phase distribution sampled on the bricks



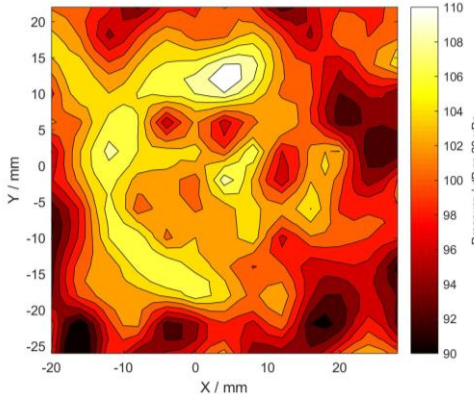
(b) Trap before displacement (COMSOL)



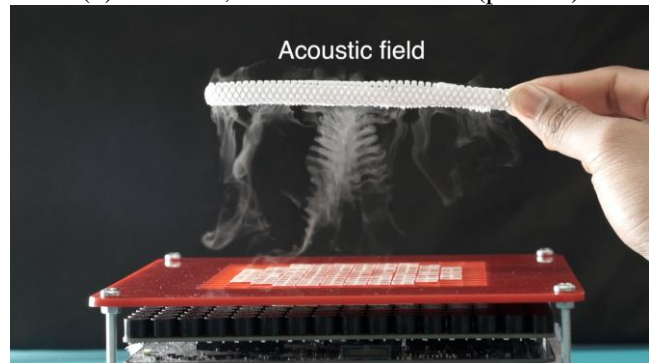
(c) XY scan, 10 mm from bricks (plane 1)



(d) XY scan, 20 mm from bricks (plane 2)



(e) XY scan, 30 mm from bricks (plane 3)



(f) Field visualisation using dry ice.

Figure 3: Characterisation of the proposed trap. (a) Phase distribution for bricks; (b) numerical simulation of sound pressure level in the vertical plane; (c-e) horizontal scans at different distances from the metasurface; (d) visualisation of the field using dry ice.

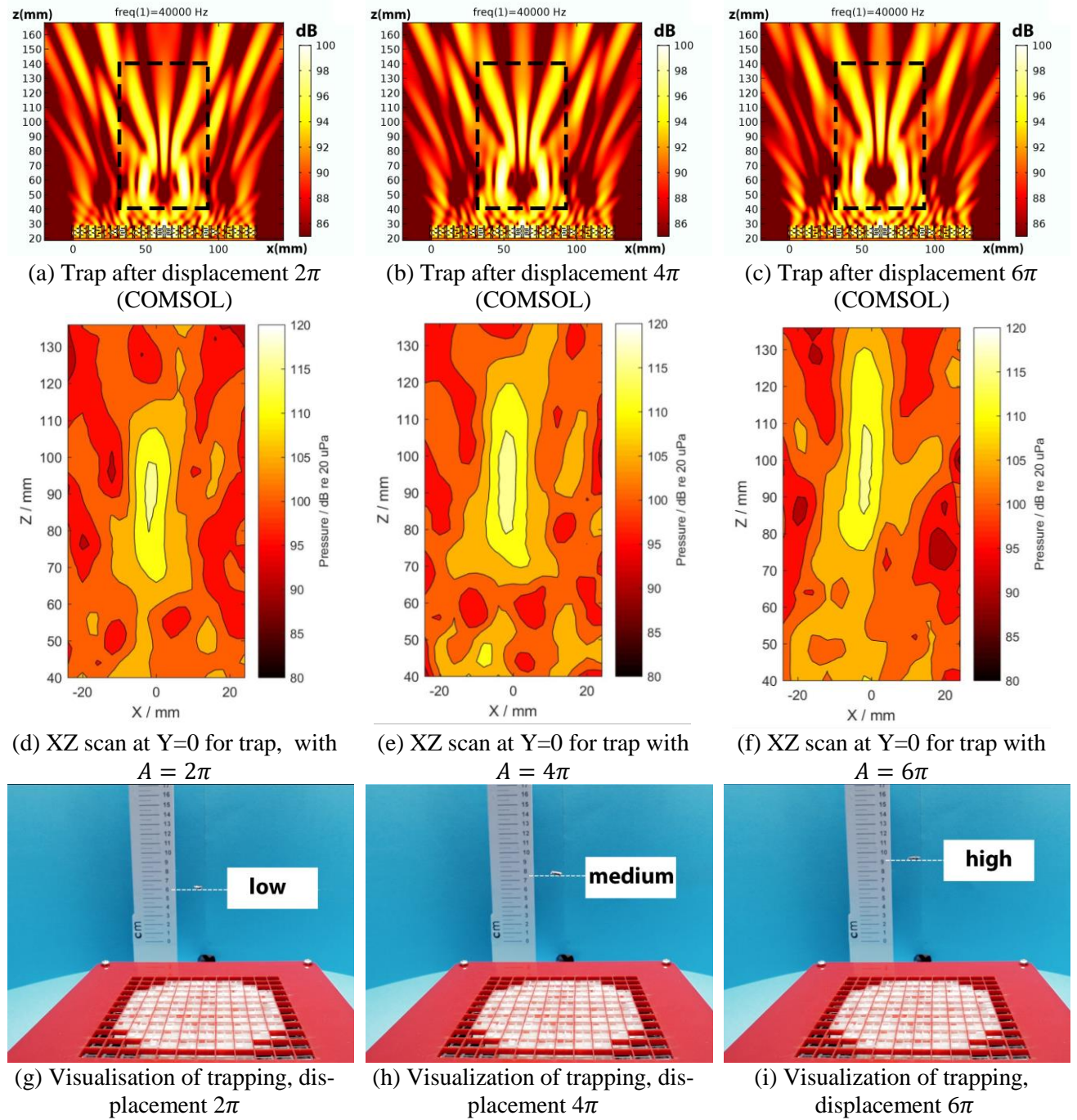

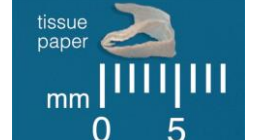



Figure 3: Generation of traps at different locations. (a-c) Numerical simulations of trap displacement; (d-f) Experimental measurements of trap displacements; (g-i) Visualisation of traps at different displacements.

Table 1: Levitation of different objects. The table reports a physical description of the object, an estimation of its density (based on a weight of 5 mg) and the distance from the meta-surface at which it levitated.

Image			
Dimension (mm)	8 x 2 x 2	5 x 2 x 2	5 x 2.5 x 1.4
Estimated density ( $\text{kg m}^{-3}$ )	156.0	250.0	286.0
Distance from the meta-surface when levitating (mm)	88	80	78

## REFERENCES

- 1 Andrade, M.A.B., Bernassau, A.L., Adamowski, J.C., Acoustic levitation of a large solid sphere, *Applied Physics Letters*, 109 (4), 44101, (2016)
- 2 Baresch, D., Thomas, J.L., Marchiano, R., Observation of a Single-Beam Gradient Force Acoustical Trap for Elastic Particles: Acoustical Tweezers, *Physical Review Letters*, 116 (2), 1–6, (2016)
- 3 Brand, E.H., Suspended by sound, *Nature*, 413 (October), 474–475, (2001)
- 4 Colombi, A., Colquitt, D., Roux, P., Guenneau, S., Craster, R. V., A seismic metamaterial: The resonant metawedge, *Scientific Reports*, 6 (1), 27717, (2016)
- 5 Cummer, S.A., Christensen, J., Alù, A., Controlling sound with acoustic metamaterials, *Nature Reviews Materials*, 1 (3), 16001, (2016)
- 6 Hertz, H.M., Standing-wave acoustic trap for nonintrusive positioning of microparticles, *Journal of Applied Physics*, 78 (8), 4845–4849, (1995)
- 7 Hoshi, T., Takahashi, M., Iwamoto, T., Shinoda, H., Noncontact tactile display based on radiation pressure of airborne ultrasound, *IEEE Transactions on Haptics*, 3 (3), 155–165, (2010)
- 8 Lee, J., Ha, K., Shung, K.K., A theoretical study of the feasibility of acoustical tweezers: Ray acoustics approach, *The Journal of the Acoustical Society of America*, 117 (5), 3273–3280, (2005)
- 9 Lee, J. Shung, K.K., Radiation forces exerted on arbitrarily located sphere by acoustic tweezer, *The Journal of the Acoustical Society of America*, 120 (2), 1084–1094, (2006)
- 10 Lin, Z., Guo, X., Tu, J., Ma, Q., Wu, J., Zhang, D., Acoustic non-diffracting Airy beam, *Journal of Applied Physics*, 117 (10), (2015)
- 11 Maldovan, M., Sound and heat revolutions in phononics, *Nature*, 503 (7475), 209–17, (2013)
- 12 Marzo, A., Ghobrial, A., Cox, L., Caleap, M., Croxford, A. en Drinkwater, B.W., Realization of compact tractor beams using acoustic delay-lines, *Applied Physics Letters*, 110 (1), 1–6, (2017)
- 13 Marzo, A., Seah, S.A., Drinkwater, B.W., Sahoo, D.R., Long, B., Subramanian, S., Holographic acoustic elements for manipulation of levitated objects, *Nature Communications*, 6 (May), 8661, (2015)
- 14 Memoli, G., Caleap, M., Asakawa, M., Sahoo, D.R., Drinkwater, B.W., Subramanian, S., Metamaterial bricks and quantization of meta-surfaces, *Nature Communications*, 8 14608, (2017)
- 15 Ochiai, Y., Hoshi, T., Rekimoto, J., Pixie Dust : Graphics Generated by Levitated and Animated Objects in, *ACM Transactions on Graphics*, 33 (4), Article 85, (2014)
- 16 Omirou, T., Perez, A.M., Subramanian, S., Roudaut, A., Floating Charts: Data Plotting using Free-Floating Acoustically Levitated Representations. *IEEE Symposium on 3D User Interfaces (3DUI)* 187–190, (2016)
- 17 Pesce, G., Volpe, G., Marago, O.M., Jones, P.H., Gigain, S., Sasso, A., Volpe, G., A Step-by-step guide to the realisation of advanced optical tweezers, 32 (5), 84–98, (2015)
- 18 Sahoo, D.R., Plasencia, D.M., Subramanian, S., Control of Non-Solid Diffusers by Electrostatic Charging. *Proceedings of the 33rd Annual ACM Conference on Human Factors in Computing Systems (CHI'15)* New York, NY, USA, 11–14, (2015)
- 19 Salter, P.S., Iqbal, Z., Booth, M.J., Analysis of the Three-Dimensional Focal Positioning Capability of Adaptive Optic Elements, *International Journal of Optomechatronics*, 7 (1), 1–14, (2013)
- 20 Sundvik, M., Nieminen, H.J., Salmi, A., Panula, P., Hæggström, E., Effects of acoustic levitation on the development of zebrafish, *Danio rerio*, embryos, *Scientific Reports*, 5 (1), 13596, (2015)
- 21 Vasileiou, T., Foresti, D., Bayram, A., Poulikakos, D., Ferrari, A., Toward Contactless Biology: Acoustophoretic DNA Transfection, *Scientific Reports*, 6 (1), 20023, (2016)
- 22 Weber, R.J.K., Benmore, C.J., Tumber, S.K., Taylor, A.N., Rey, C.A., Taylor, L.S., Byrn, S.R., Acoustic levitation: Recent developments and emerging opportunities in biomaterials research, *European Biophysics Journal*, 41 (4), 397–403, (2012)
- 23 Xie, W.J., Cao, C.D., Lü, Y.J., Hong, Z.Y., Wei, B., Acoustic method for levitation of small living animals, *Applied Physics Letters*, 89 (21), 214102, (2006)
- 24 Zhang, P., Li, T., Zhu, J., Zhu, X., Yang, S., Wang, Y., Yin, X., Zhang, X., Generation of acoustic self-bending and bottle beams by phase engineering., *Nature communications*, 5 4316, (2014)
- 25 Zhang, S., Xia, C., Fang, N., Broadband Acoustic Cloak for Ultrasound Waves, 24301 (January), 1–4, (2011)
- 26 Zhao, S., A standing wave acoustic levitation system for large planar objects, 7624164 (81), 123–139, (2011)
- 27 Zigoneanu, L., Popa, B., Cummer, S.A., Three-dimensional broadband omnidirectional acoustic ground cloak, *Nature materials*, 13 (March), 1–4, (2014)